A STABILISED FINITE ELEMENT METHOD FOR MODELLING FLUID FLOW AND CONTAMINANT MIGRATION IN GEOSYNTHETICS

Abbas El-Zein, Parnel Richards and Nigel Balaam
School of Civil Engineering, University of Sydney, NSW 2006, Australia

A stabilised Petrov-Galerkin Laplace finite element method (SLFEM) for the modelling of flow and contaminant transport in multi-layered containment systems comprising a geosynthetic clay liner (GCL) is developed. The method determines the hydraulic regime as well as the time-dependent transport of contaminants in the system. It can accurately represent the sudden jump in Darcy velocities close to leaks in the geomembrane. It is implemented in the computer software, Soil Pollution Analysis System (SPAS) with an easy-to-use graphic interface. The coupled equations of flow and transport are first presented, as well as the SLFEM formulation. The main features of SPAS are described and a case study of the transport of trichloroethene in a single composite liner is analysed. Finally, the usefulness of SPAS and more generally concentration-based assessments of geosynthetic liners in 2D space is discussed.

1 INTRODUCTION

Low-permeability geosynthetics are now widely used as barriers against the migration of contaminants from pollution sources (Rowe, 2005). They have been shown to be often more cost-effective than conventional compacted clay liners. However, in many statutes, the onus is on the landfill designer to show that the geosynthetics-based liner design is "equivalent" to the one prescribed by the regulations. Modelling hence becomes an important part of the design process, needed to establish equivalency (Rowe and Brachman, 2004). While 1D models can be used to simulate fluid flow and contaminant migration, they are incapable of fully capturing many of the important features of the system, such as groundwater flow and leakage through geomembranes, and can lead to overly conservative or unsafe results (El-Zein, 2008; El-Zein and Rowe, 2008). On the other hand, the thinness of geosynthetics layers introduces a new scale into the analysis and sharp concentration fronts near the edge of geomembrane defects, adding a level of complexity to the simulation exercise. Specifically, a relatively low transmissivity reflecting good contact between the geomembrane and the GCL leads to a sudden jump in vertical Darcy velocity near the leaks. This near-discontinuity is difficult to model for two reasons. First, it requires careful mesh refinement to capture the sudden jump. Second, the high Peclet numbers (reflecting large advection relative to diffusion) introduce oscillations around the real solution (Zienkiewicz and Taylor, 1991; Franca *et al*., 1992).

We present a stabilized Laplace-transform finite-element method (SLFEM) for simulating fluid flow and contaminant transport in multilayered landfill liners including geosynthetics or compacted clay liners. The novelty lies in applying the Petrov-Galerkin stabilisation technique to the Laplace finite element method and removing numerical oscillations resulting from high Peclet numbers. Stabilisation has been previously applied to time-domain methods but not Laplace-domain ones. The Laplace-domain methods are faster and simpler to use because they do not require time stepping. The method has been implemented in a computer software called Soil Pollution Analysis System (SPAS) developed earlier at the University of Sydney. The software has an easy-to-use graphic interface for rapid model construction and result viewing. SPAS offers three major advantages over conventional approaches:

a) it allows a more faithful representation of relevant transport and partitioning processes;
b) it calculates the leakage rates in the liners more accurately than 1D based approximations commonly used by the landfill-design engineers;
c) it allows a more accurate assessment of equivalency that is based on maximum chemical concentrations of pollutants in the aquifer, rather than hydraulic leakage rates through the liners.

The use of automatically-generated meshing configurations tailored specifically for geosynthetics is especially important in SPAS. Features such as diffusion and advection through the various layers of the liner, sorption, surface sorption on the geomembrane, biological or radioactive decay, flow and dispersion in the aquifer, transmissive layers to represent imperfect contact between the geomembrane and the top of the clay liner, conserved mass of contaminants in the waste, and advective discharge at the boundaries are all included.

In the remainder of this paper, we present the equations of coupled seepage flow and mass transport, as well as the stabilised Petrov-Galerkin finite element formulation. Next, the main features of SPAS are briefly described. The case of

transport of trichloroethene (TCE) through a GCL is studied and a parametric analysis is performed to assess the effects of various design variables on leakage rates and contaminant concentrations in the groundwater. Finally, the implications of a chemical-concentration based assessment of the equivalency of geosynthetics is discussed.

2 STABILISED LAPLACE TRANSFORM FINITE-ELEMENT METHOD FOR COUPLED FLUID FLOW AND CONTAMINANT TRANSPORT PROBLEMS

The time-dependent seepage equation is based on Darcy's theory of fluid flow. It simulates the movement of water in the soil. In 2D space, it can be written as:

$$\frac{\partial}{\partial x}\left(k_{xx}\frac{\partial H}{\partial x}\right)+\frac{\partial}{\partial y}\left(k_{xy}\frac{\partial H}{\partial x}\right)+\frac{\partial}{\partial x}\left(k_{yx}\frac{\partial H}{\partial y}\right)+\frac{\partial}{\partial y}\left(k_{yy}\frac{\partial H}{\partial y}\right)=S_h\frac{\partial H}{\partial t} \quad \textbf{(1)}$$

where x (L) and y (L) are the dimensions of a Cartesian coordinate system;t (T) is time (t>0); H (L) is the total pressure head; k_{xx} ($L.T^{-1}$), k_{xy} ($L.T^{-1}$), k_{yx} ($L.T^{-1}$) and k_{yy} ($L.T^{-1}$) are elements of the tensor of hydraulic conductivity ($k_{xx}>0$, $k_{xy}\geq 0$, $k_{yx}\geq 0$, $k_{yy}>0$); and S_h (L^{-1}) is the coefficient of specific storage, also referred to as specific yield ($S_h>0$);

If H(t,x,y) is known, the components of the seepage velocity, v_x and v_y, can be calculated from the following equations:

$$v_x=-\frac{k_{xx}}{n}\frac{\partial H}{\partial x} \quad \textbf{(2)}$$

$$v_y=-\frac{k_{yy}}{n}\frac{\partial H}{\partial y} \quad \textbf{(3)}$$

where n is the soil porosity. The components of the Darcy velocity can be obtained from the following equations:

$$v_{ax}=nv_x \quad \textbf{(4)}$$

$$v_{ay}=nv_y \quad \textbf{(5)}$$

The time-dependent reactive diffusion-advection equation can be written as:

$$\prod(c)=(n+\rho K_d)\frac{\partial c}{\partial t} \quad \textbf{(6)}$$

$$\prod(c)=n\frac{\partial}{\partial x}\left(D_{xx}\frac{\partial c}{\partial x}\right)+n\frac{\partial}{\partial x}\left(D_{xy}\frac{\partial c}{\partial y}\right)+n\frac{\partial}{\partial y}\left(D_{yx}\frac{\partial c}{\partial x}\right)+n\frac{\partial}{\partial y}\left(D_{yy}\frac{\partial c}{\partial y}\right)-nv_x\frac{\partial c}{\partial x}-nv_y\frac{\partial c}{\partial y}-n\lambda c$$

where c(t,x,y)($M.L^{-3}$) is the concentration of dissolved contaminant in soil water ($c\geq 0$); D_{xx} ($L^2.T^{-1}$), D_{xy} ($L^2.T^{-1}$), D_{yx} ($L^2.T^{-1}$) and D_{yy} ($L^2.T^{-1}$) are elements of the tensor of hydrodynamic dispersion ($D_{xx}>0$, $D_{yx}>0$, $D_{xy}>0$, $D_{yy}>0$);v_x ($L.T^{-1}$) and v_y ($L.T^{-1}$) are the components of seepage velocity calculated from equations (1), (2) and (3); ρ ($M.L^{-3}$) is the dry density of the soil ($\rho>0$); K_d ($L^3.M^{-1}$) is the linear instantaneous sorption distribution coefficient ($K_d\geq 0$);λ (T^{-1}) is the coefficient of first-order, rate-limited decay ($\lambda\geq 0$), more conveniently expressed by the decay half-life $t_{½}$ (T) where $\lambda=\ln(2)/t_{½}$ and ln is the natural logarithm.

Equation (6) simulates the fate of a chemical species, dissolved in the soil's water, subject to diffusion, mechanical dispersion, advective flow, linear instantaneous sorption and first-order decay. Diffusion and dispersion are assumed to follow Fick's laws of diffusion. The coefficients of hydrodynamic dispersion represent both molecular diffusion and mechanical dispersion in the soil. They can be evaluated using the following equations:

$$D_{xx}=\alpha_T|v|+(\alpha_L-\alpha_T)\frac{v_x^2}{|v|} \quad \textbf{(7)}$$

$$D_{xy}=(\alpha_L-\alpha_T)\frac{v_xv_y}{|v|} \quad \textbf{(8)}$$

$$D_{yy}=\alpha_T|v|+(\alpha_L-\alpha_T)\frac{v_y^2}{|v|} \quad \textbf{(9)}$$

where α_T (L) and α_L (L) are the transverse and longitudinal dispersivities, respectively ($\alpha_T \geq 0$ and $\alpha_L \geq 0$) and $|v| = \sqrt{v_x^2 + v_y^2}$. If c is known, the fluxes of contaminants f_x ($M.L^{-2}.T^{-1}$) and f_y ($M.L^{-2}.T^{-1}$) can be calculated using the following equations, based on Fick's first law of diffusion:

$$f_x = -nD_{xx}\frac{\partial c}{\partial x} + nv_x c \quad \textbf{(10)}$$

$$f_y = -nD_{yy}\frac{\partial c}{\partial y} + nv_y c \quad \textbf{(11)}$$

As stated above, conventional finite element method (FEM) solutions of the diffusion-advection equation suffer from numerical oscillations around the real solution. Here, a stabilisation technique, known as the Streamline Petrov-Galerkin method and previously used with steady-state and time-domain approaches, is applied to the Laplace-transform finite element formulation. It consists of modifying the weighing functions in the discretised finite element residual statement as follows:

$$\sum_{e=1}^{N}\left[\int_{\Omega_e} N_i^e(x,y)\{\Pi(\bar{c}) - s\bar{c}\}d\Omega_e\right] = 0 \quad \textbf{(12)}$$

where $\bar{c}$ is the Laplace transform of c, N is the number of elements, Ω_e is the element domain and $N_i^e(x,y)$ is the modified shape function:

$$N_i^e(x,y) = N_i^e + \frac{\alpha h}{2}\frac{v_x\frac{\partial N_i^e}{\partial x} + v_y\frac{\partial N_i^e}{\partial y}}{|v|} \quad \textbf{(13)}$$

where N_i^e are the original (polynomial) shape functions, usually linear or quadratic; h is a representative length of the element in the direction of seepage; α is determined heuristically to remove oscillations ($\alpha = \coth P_e - 1/P_e$.for the steady-state problem with no reactive term) (Franca *et al*., 1992). Equation (12) can be integrated by parts to obtain a weak formulation which forms the basis of a finite element algorithm. Discretisation of the equation yields an algebraic system equation which can be solved to derive the nodal Laplace transformed concentrations. The solution is inverted numerically into the time domain.

3 SOIL POLLUTION ANALYSIS SYSTEM (SPAS) FOR TRANSPORT IN GCLS

The stabilized Laplace-transform finite-element method presented above has been implemented in the Soil Pollution Analysis System (SPAS). SPAS is suited for the analysis of a number of seepage and contaminant problems. It can solve the steady-state or transient seepage and reactive mass transport equations of single species in saturated soils under single, double and multiple-porosity chemical conditions. In addition, SPAS solves the coupled steady-state seepage and time-dependent mass transport equations. It is especially useful for analysing seepage and contaminant migration through multi-layered landfill liners, including those with leaking geomembranes. Features such as primary and secondary liners, multiple leaks, symmetry, inclinations, slopes, transmissive layers between geomembranes and clay liners, and mass-conserving boundary conditions are easily incorporated in the models. SPAS contains 3-noded, 4-noded, 6-noded and 8-noded, linear and quadratic elements. In order to minimise execution time. it uses two different Laplace transform inversion algorithms, depending on number of time stations at which the solution is required. Figure 1 shows the top menu of SPAS which takes the user through a simple step-by-step procedure to enter the data.

GCLs are used in landfill liners because of their low hydraulic conductivities, good contact properties with the overlying geomembrane as well as their relative ease of handling. However, the first two properties generate sharp advective fronts whenever a leak is present in the geomembrane (see Figure 2a). Such fronts are also present in CCLs. However, they are spread over a larger surface area because of the poorer contact properties of CCLs (see Figure 2b) which increases leakage rates. While this is a geoenvironmental advantage for the GCLs, it makes the Arrow modelling exercise more complex. To deal with this, SPAS provides two levels of refinement in order to accurately model the sudden jump in Darcy velocity. Figure 3 shows a typical refined mesh and Figure 4 shows the SPAS menu that allows the user to control the mesh generated. SPAS also provides default mesh generation control values which automatically generate refinement around the leaks.

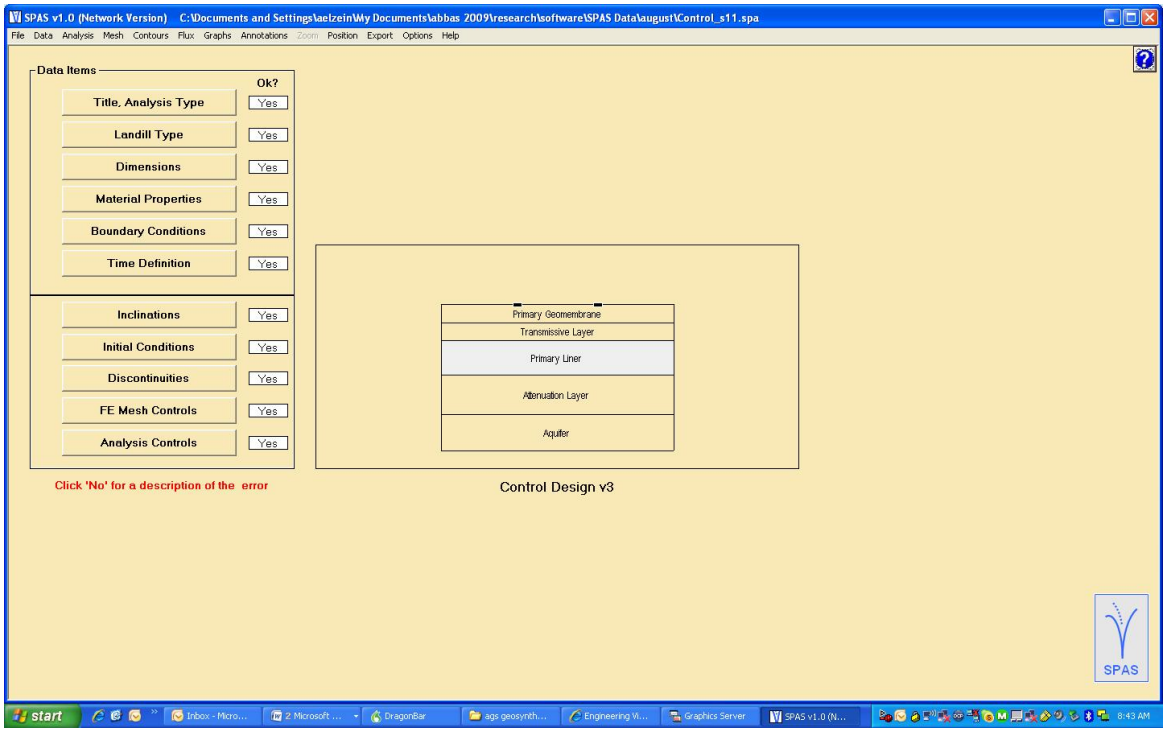

Figure 1: SPAS top menu, also showing a cross-section of the problem analysed in this paper (layers not to scale).

4 TRANSPORT OF TRICHLOROETHENE IN A GCL

Trichloroethene, also known as trichloroethylene (C_2HCl_3), is an industrial solvent which, despite its short half-life in the environment, has been previously found in groundwater. Table 1 shows the material properties used in the SPAS analyses. In addition to a base case, the effects of the variability of 8 parameters have been assessed: thicknesses of the geomembrane, GCL and the attenuation layer; the hydraulic conductivities of the GCL and the attenuation layer; the width and frequency of the leaks in the geomembrane and the transmissivity of the geomembrane-GCL interface. Given the fast biodegradation rates of trichloroethene, a factor of safety of 4 was applied. Note that the purpose of the exercise is to assess the effects of the above parameters with respect to a base case. Hence, the actual concentrations calculated are of less interest than their sensitivity to the relevant parameters. The different layers represented in the model are shown in Figure 1. A finite mass of contaminant is applied as a boundary conditions representing trichloroethene in the waste. An advective discharge boundary condition ($f_x=nv_xc$) is applied on the right-hand side vertical edge of the aquifer. The hydraulic pressure on top of the liner and in the aquifer are taken to be 300 mm and 2.75 m, respectively.

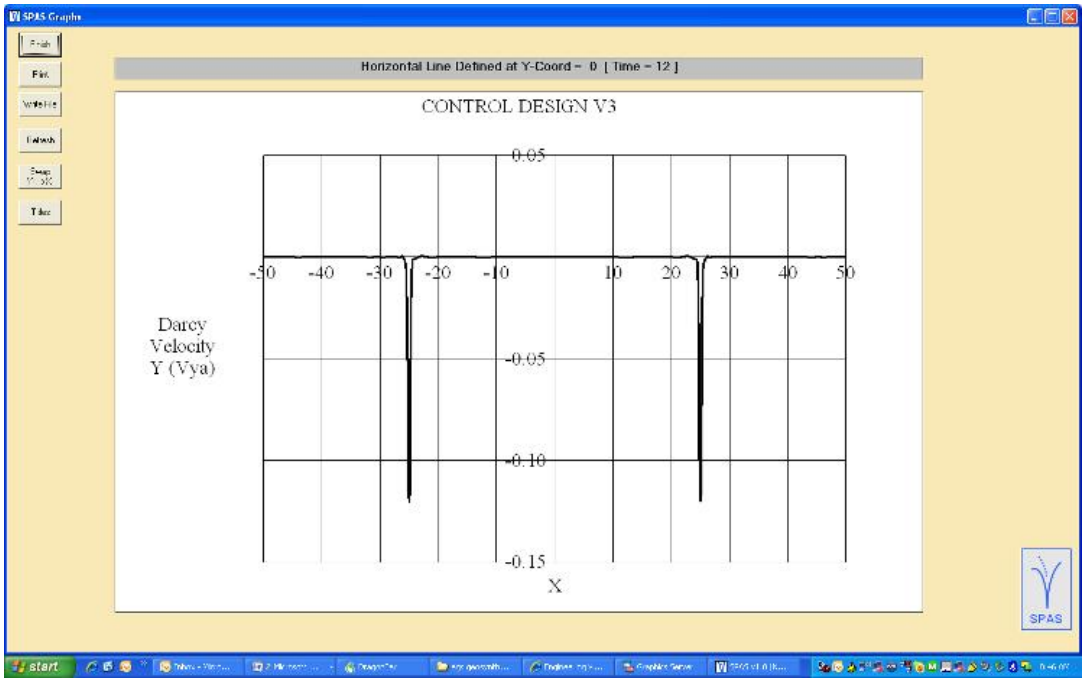

a. GCL (7 mm thick, $k_{xx}=k_{yy}=5x10^{-11}$ m/s; transmissivity=10^{-10} m^2/s)

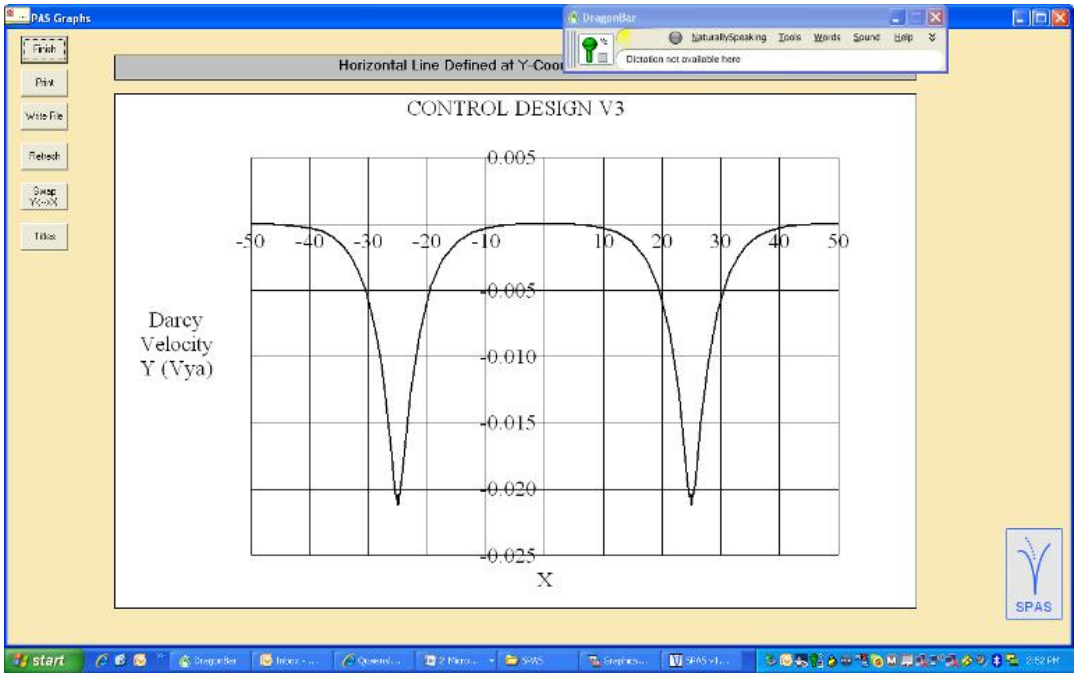

b. CCL (750 mm thick, $k_{xx}=k_{yy}=10^{-9}$ m/s; transmissivity=$1.6x10^{-8}$ m^2/s)

Figure 2: Sudden jump in vertical Darcy velocities near the leaks at the base of the GCL in a two-leak problem (the case of a CCL is shown for comparison)

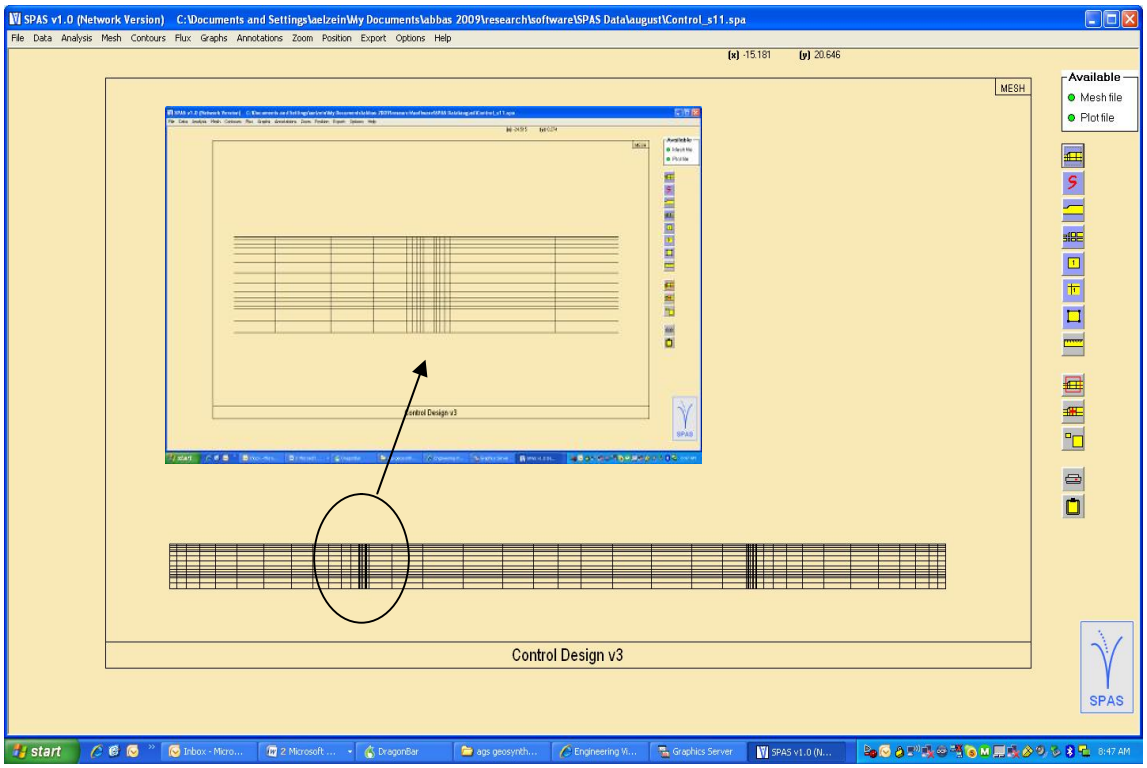

Figure 3: Automatically generated Finite-Element mesh for a two-leak problem with double selective refinement around the leaks: extra row of elements next to the leak + gradual refinement approaching the leak region.

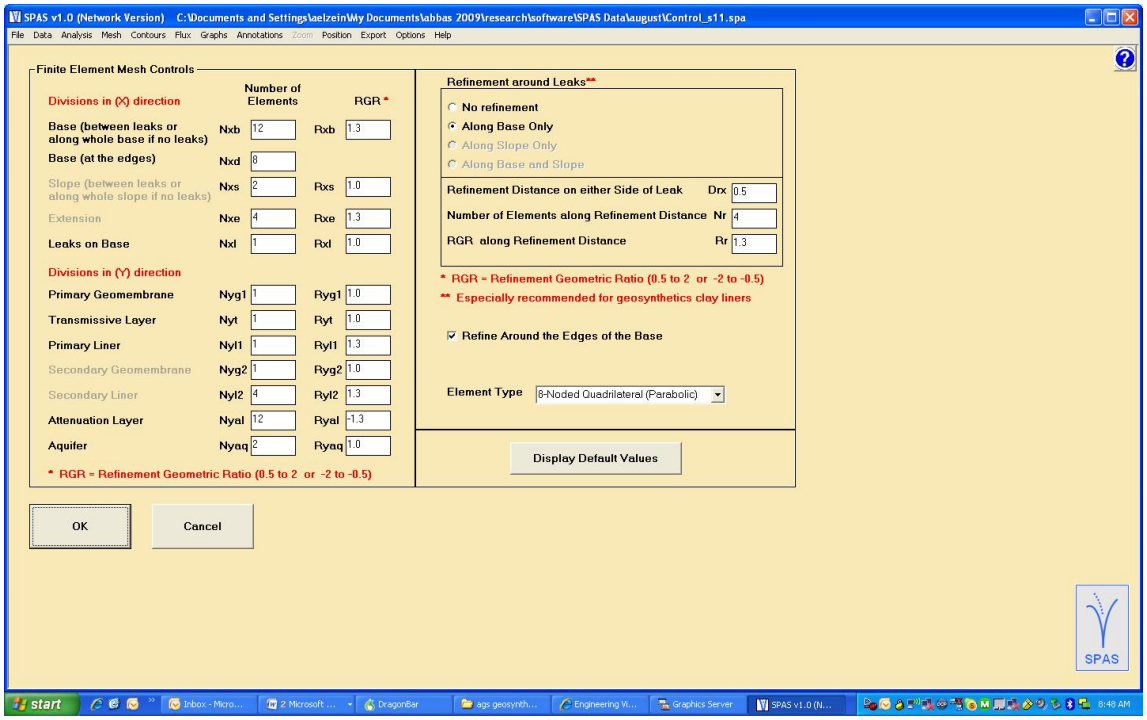

Figure 4: SPAS Finite-Element mesh control menu.

Table 1: Dimensions, material properties and parameters for the contaminant trichloroethene (TCE).

Layer	Entity	Symbol	Units	Value	Range	Source
Waste	length of base cell	L	m	100		
	waste per unit area	d_w	t/m^2	25		a
	proportion in the waste	p	mg/kg	0.59		b
	initial concentration	C_o	µg/L	400		b
	equivalent height of leachate	H_r	m	36.875		
	decay half-life	$t_{1/2g}$	years	1.2		c
Geomembrane	thickness	h	mm	1.5	1-2.5	
	diffusion coefficient	D_g	m^2/s	$4x10^{-13}$		b
	partition coefficient	S_{gf}	DL[1]	85		b
	transmissivity	θ	m^2/s	10^{-10}	10^{-11}-10^{-9}	
	decay half-life	$t_{1/2}$	years	no decay		
	wrinkle width	w	m	0.3	0.1-0.5	
	wrinkle frequency	F	/ha	2.5	0-4	
	total hydraulic head	H	m	3.3		
Transmissive Layer	thickness	h	mm	0.1		
GCL	thickness	h	mm	7	5-12	b
	porosity	n	DL	0.7		
	hydraulic conductivity	k_{xx}, k_{yy}	m/s	$5x10^{-11}$	$5x10^{-12}$ - $6x10^{-11}$	b
	diffusion coefficient	D_o	m^2/s	$3x10^{-10}$		b
	decay half-life	$t_{1/2}$	years	8.4		c
Attenuation Layer	thickness	h	m	3	1-5	
	porosity	n	DL	0.35		
	hydraulic conductivity	k_{xx}, k_{yy}	m/s	10^{-7}	10^{-8}-10^{-6}	
	diffusion coefficient	D_o	m^2/s	$6x10^{-10}$		
	decay half-life	$t_{1/2}$	years	8.4		
Aquifer	thickness	h	m	1		
	porosity	n	DL	0.3		
	hydraulic conductivity	k_{xx}, k_{yy}	m/yr	∞		
	hydrodynamic dispersion	D_{xx},D_{yy}	m^2/year	100		
	Darcy velocity	v_{xa}	m/s	1		
	decay half-life	$t_{1/2}$	years	8.4		
	total hydraulic head at base	H	m	2.75		

[1]DL: dimensionless;
[a]El-Zein and Rowe (2008)
[b]Rowe *et al.* (2004)
[c]CCM (2007)

5 RESULTS

SPAS results have been validated by comparing its predictions to those of a range of analytical and numerical solutions. These included the Ogata-Banks equation (Ogata and Banks, 1961), the Booker Rowe equation (Booker and Rowe, 1987), a finite-layer method (Rowe and Booker, 1984) and a boundary element method (El-Zein, 2003). Another validation process has aimed at checking the effect of stabilisation and confirm that it does indeed remove oscillations around the real solution. Figure 5 shows results from such a process where oscillations apparent in the Galerkin FEM are clearly dampened in the profiles produced by SLFEM. The full validation results will not be presented here. Instead, for the sake of brevity, we will focus exclusively in this section on the analysis of trichloroethene transport.

Figures 6 to 8 show concentration distributions in space and time for the baseline case. In the aquifer, concentrations are higher towards the right-hand side as a result of rightward water flow. However, this is mitigated by the dilution effects of mechanical dispersion taken as 100 m^2/year. Results of parametric analyses are shown in Table 2 as well as Figures 9 to 16. Two aspects of the results are noteworthy: a) the sensitivity of leakage rates and concentrations of trichloroethene in groundwater to the parameters in question and b) the extent to which leakage rates and concentrations exhibit the same patterns of sensitivity to the studied parameters.

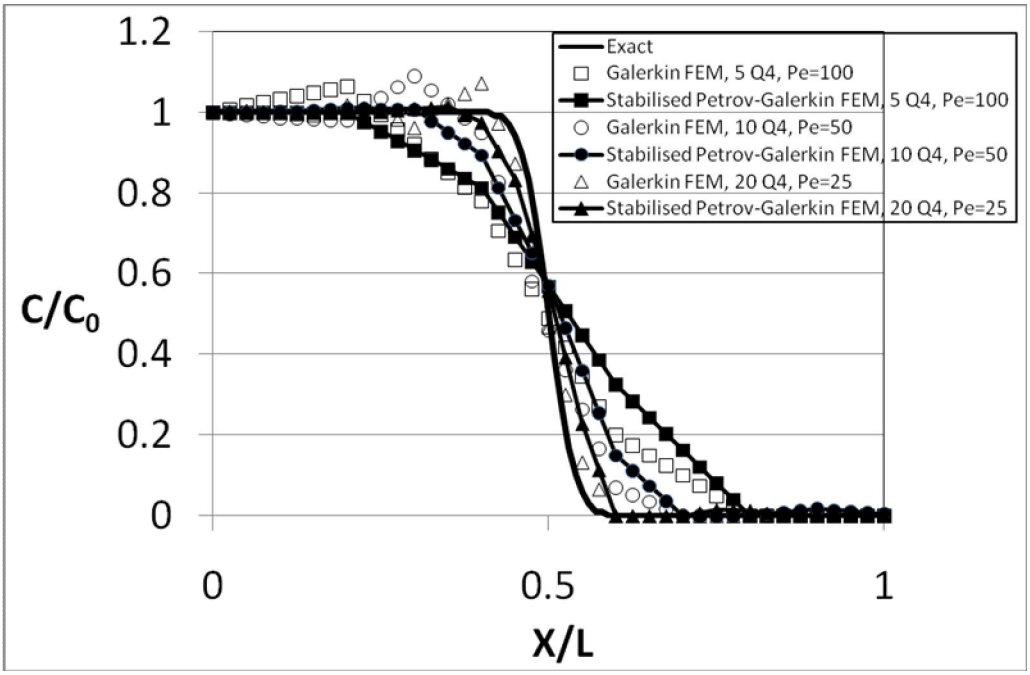

Figure 5. Effect of stabilisation: results for a 1D advection-dominated case ($D_{xx}=10^{-5}m^2.year^{-1}$, v_x=-0.01 $m.year^{-1}$, t=50 years, α=1; Q4 is a four-noded linear quadrilateral element; $P_e=vL_{xe}/(2D_{xx})$ and L_{xe} is the length of the element)

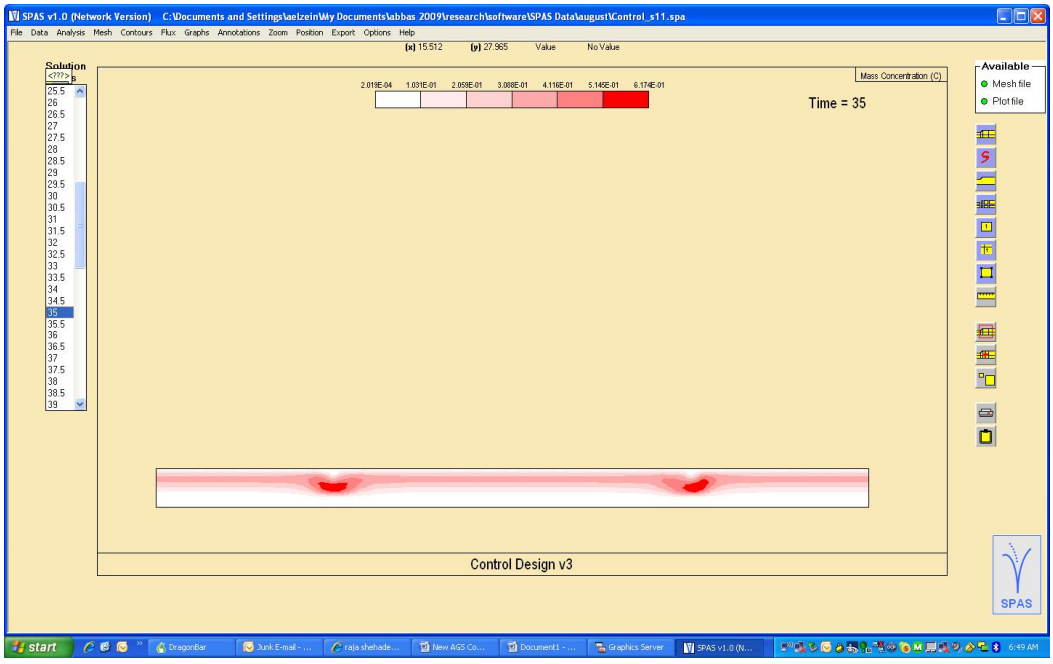

Figure 6: Baseline case: contours of trichloroethene concentrations at t = 35 years.

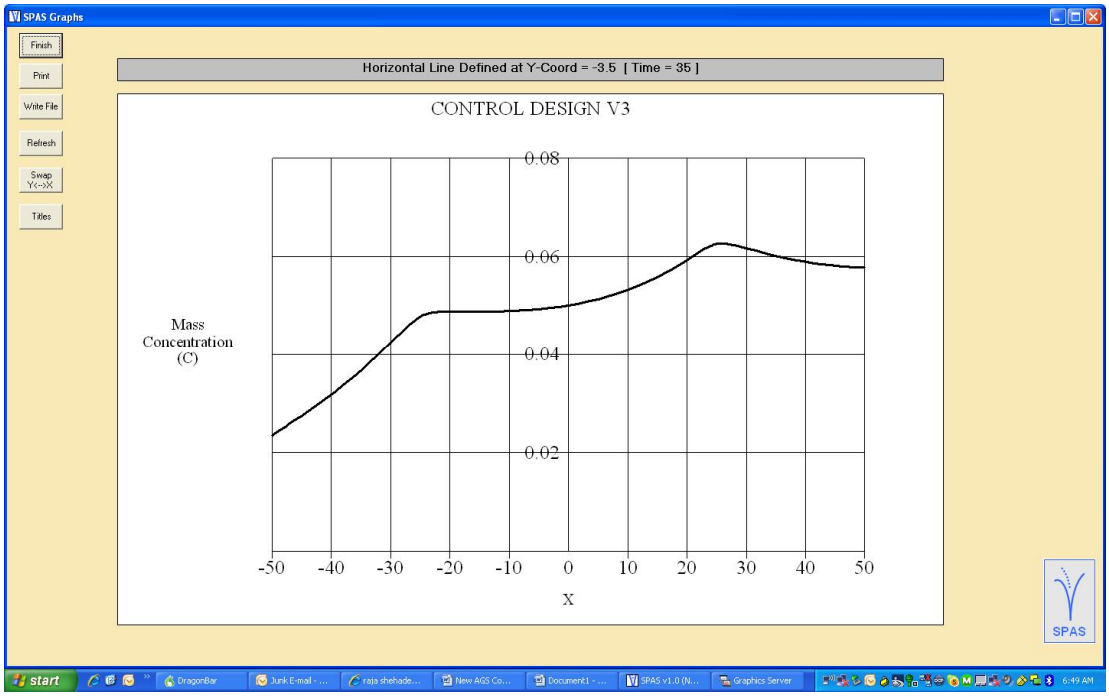

Figure 7: Baseline case: horizontal profile of trichloroethene concentrations at t = 35 years in the aquifer.

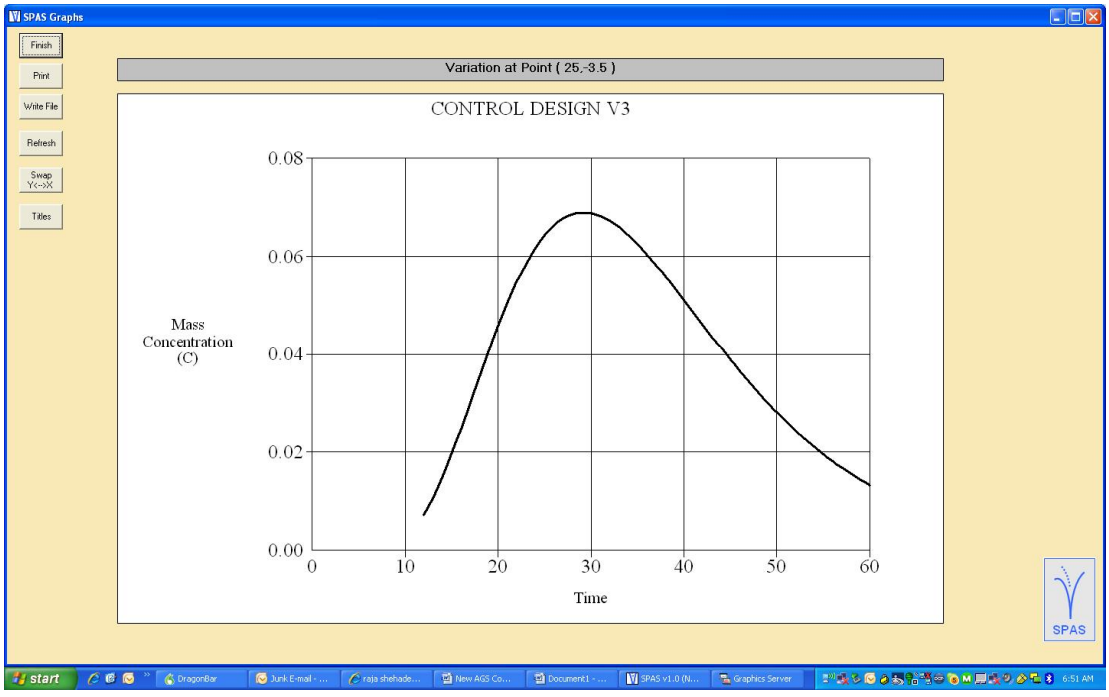

Figure 8. Base case: concentration versus time in the aquifer under the rightmost leak.

Table 2: Summary of results (baseline case is shown in bold-faced characters)

Parameter	Units	Value	Results	
			Leakage Rate[1]	Concentration[2]
			lpdh	C/C_o x 10^{-4}
Number of Leaks		0	0.00	0.62
		1	17.81	1.34
		2	**35.95**	**1.71**
		3	52.60	1.97
		4	70.38	2.26
		5	88.27	2.71
Leak Width	m	0.1	22.05	1.09
		0.2	28.99	1.41
		0.3	**35.95**	**1.71**
		0.4	42.22	2.14
		0.5	47.70	2.66
Geomembrane Thickness	mm	1	35.92	1.72
		1.5	**35.95**	**1.71**
		2	35.89	1.70
		2.5	35.86	1.68
GCL Thickness	mm	5	45.56	2.46
		7	**35.07**	**1.71**
		10	27.67	1.27
		12	24.50	1.13
Attenuation Layer Thickness	m	1	36.05	99.00
		2	36.22	11.55
		3	**35.95**	**1.71**
		4	35.73	0.28
		5	35.89	0.05
Transmissivity	m^2/s	10^{-12}	21.89	1.08
		10^{-11}	25.24	1.20
		10^{-10}	**35.95**	**1.71**
		$5x10^{-10}$	56.52	3.21
		10^{-9}	72.41	4.82
GCL Hydraulic Conductivity	m/s	$5x10^{-12}$	7.82	0.71
		10^{-11}	11.89	0.78
		$2x10^{-11}$	18.86	0.95
		$3x10^{-11}$	24.59	1.15
		$4x10^{-11}$	30.36	1.41
		$5x10^{-11}$	**35.95**	**1.71**
		$6x10^{-11}$	40.71	2.05
Attenuation Layer Hydraulic Conductivity	m/s	10^{-8}	26.58	1.25
		$5x10^{-8}$	34.49	1.63
		10^{-7}	**35.95**	**1.71**
		$5x10^{-7}$	36.90	1.78
		10^{-6}	37.18	1.79

1 Hydraulic Leakage Rate calculated at the base of the GCL in litres per day per hectare;
2 Peak concentrations of TCE in the aquifer as a proportion of the initial concentration in the waste (C_o = 400 μg/L)

Figures 9 and 10 show that, as expected, leakage and contamination increase with increasing frequency and size of leaks. It is clear from Figure 11 that the geomembrane thickness plays a negligible role in the presence of leaks. This is because the rate of transfer of contaminants from the waste repository is controlled by the leaking rather than the intact parts. The thickness of the GCL appears to be far more important than that of the attenuation layer in reducing the leakage rates (Figures 12 and 13). However, chemical concentrations in groundwater are highly sensitive to the thickness of the attenuation layer because the latter provides a diffusion buffer against contaminant transport (Figure 13). Both the hydraulic conductivity of the GCL (Figure 14) and the transmissivity of the GCL-Geomembrane interface (Figure 16) have a significant effect on the hydraulic and chemical performances of the liner. Figure 15 shows that the change in leakage rates and concentrations as the hydraulic conductivity of the attenuation layer varies is close to logarithmic. It also shows that little gain is achieved by reducing the hydraulic conductivity of the attenuation layer from 10^{-6} m/s to around $2x10^{-7}$ m/s while more significant drops in leakage rates and concentrations are observed beyond the value of $2x10^{-7}$ m/s.

Comparing trends of leakage rates to those of chemical concentrations, it is evident that the two do not always follow the same patterns. For example, compared to leakage rates, concentrations grow more slowly with number of leaks per hectare but faster with width of leaks and hydraulic conductivity of the GCL. More significantly, as discussed above, the thickness of the attenuation layer has a strong impact on the concentrations but appears to have little influence on the leakage rates in the studied ranges.

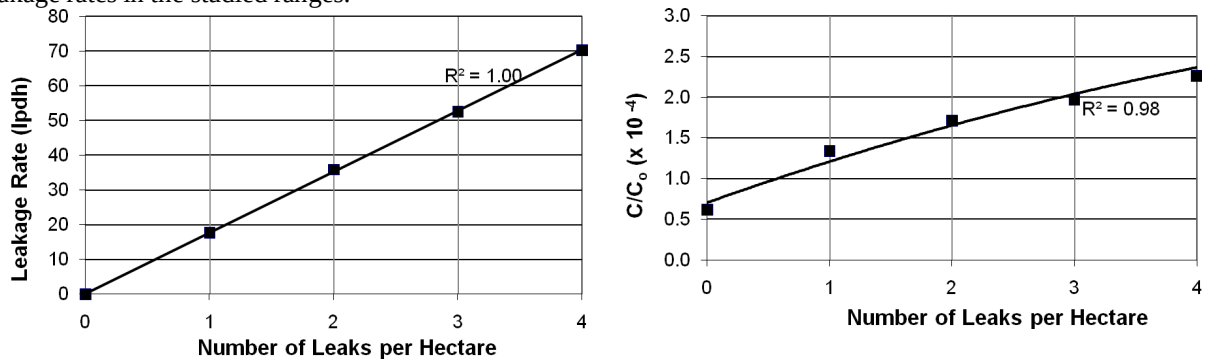

Figure 9: Effects of leak frequency (trendlines: linear for leakage rate and parabolic for C/C_0)

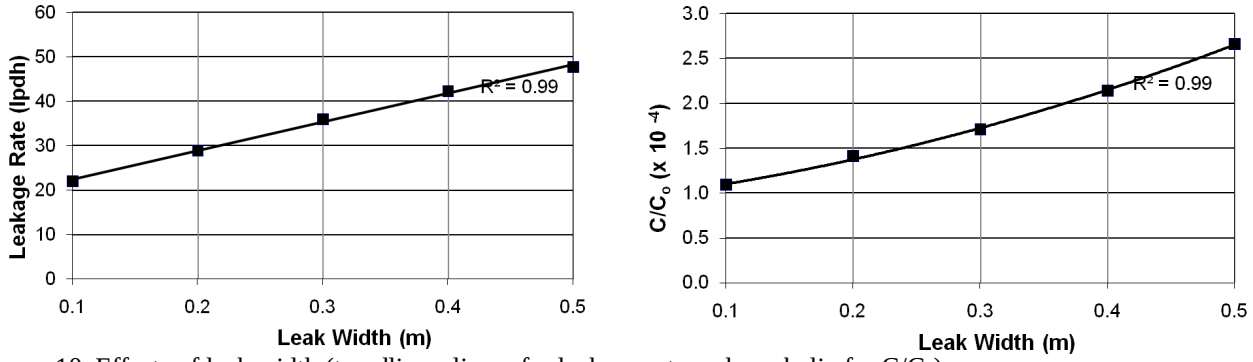

Figure 10: Effects of leak width (trendlines: linear for leakage rate and parabolic for C/C_0)

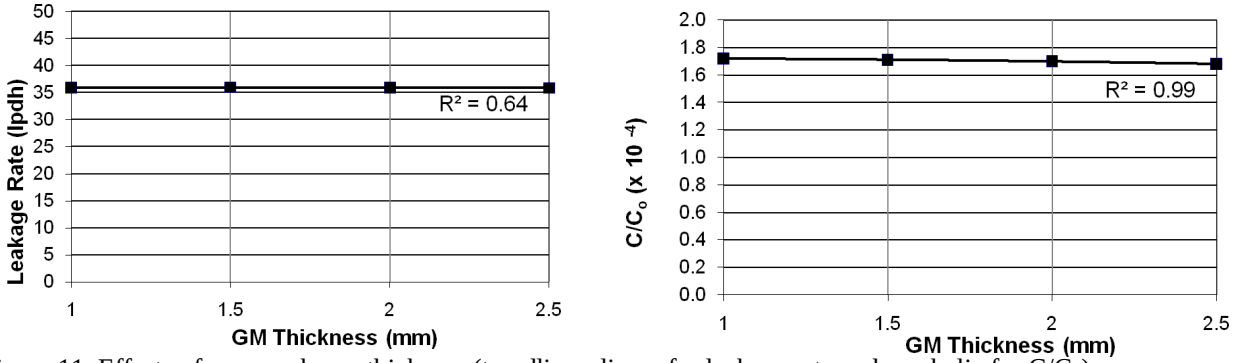

Figure 11: Effects of geomembrane thickness (trendlines: linear for leakage rate and parabolic for C/C_0)

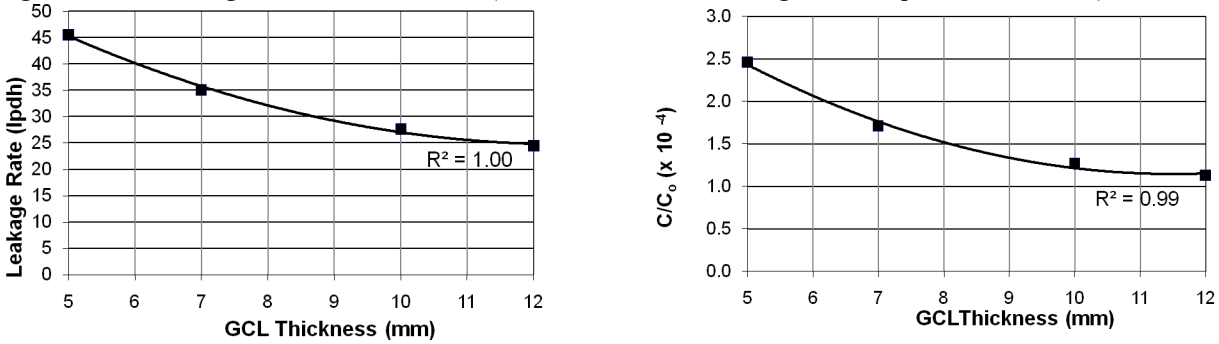

Figure 12: Effects of GCL thickness (parabolic trendlines).

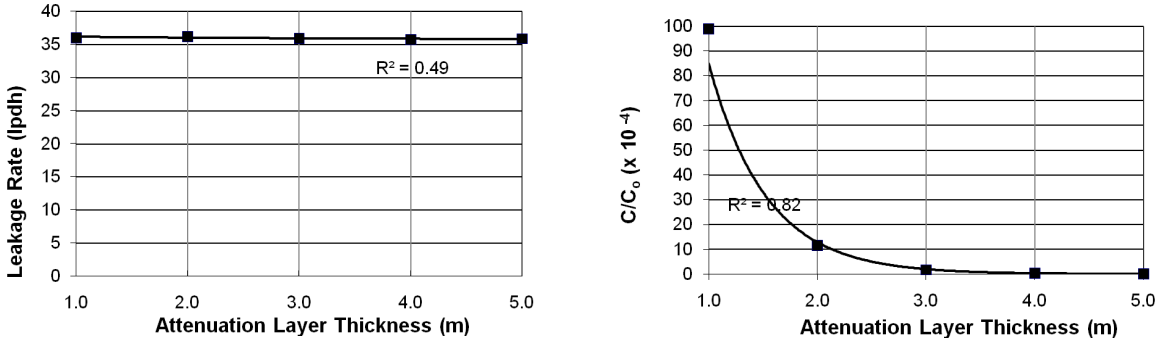

Figure 13: Effects of attenuation-layer thickness (trendlines: linear for leakage rate and parabolic for C/C_0)

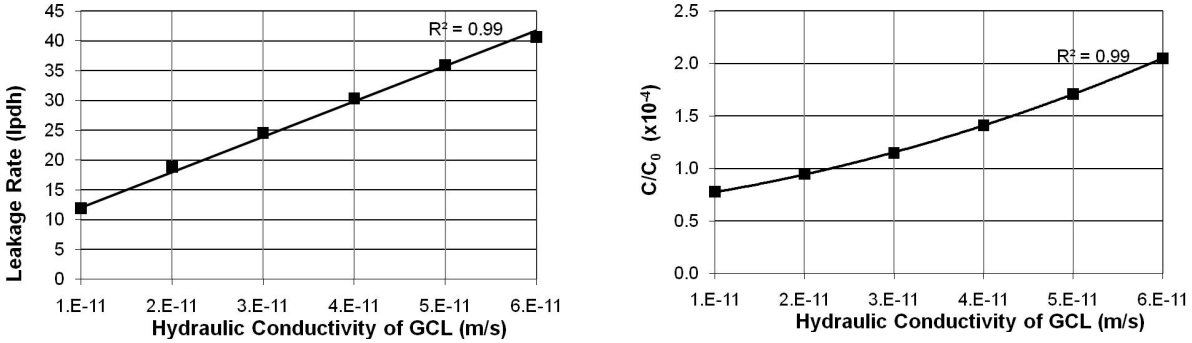

Figure 14: Effects of GCL hydraulic conductivity (trendlines: linear for leakage rate and parabolic for C/C_0)

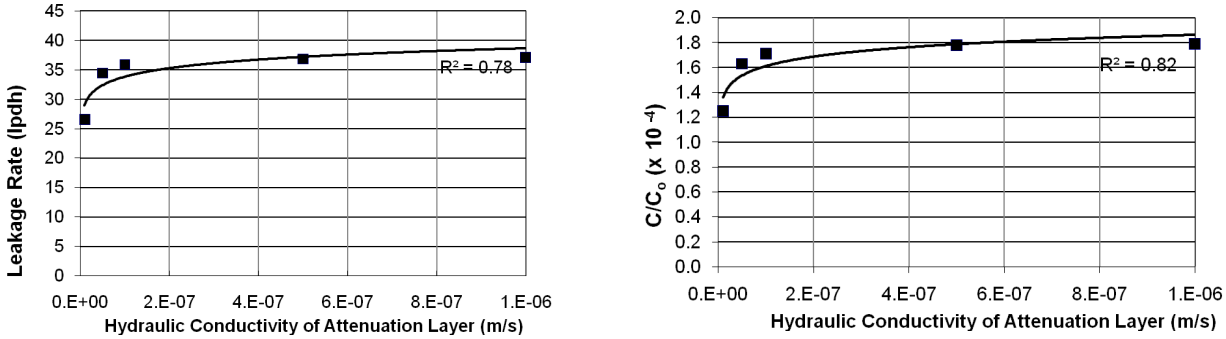

Figure 15: Effects of hydraulic conductivity of attenuation layer (logarithmic trendlines)

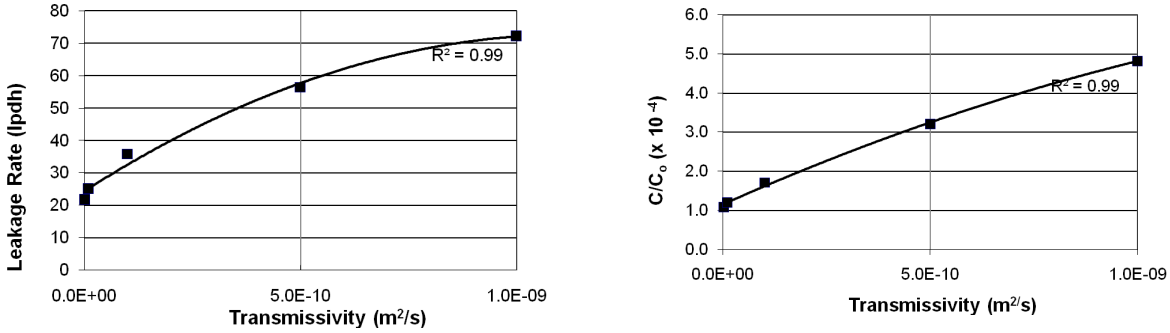

Figure 16: Effects of geomembrane-GCL transmissivity (parabolic trendlines).

The kind of sensitivity analyses performed here is important for two reasons. Firstly, they give a measure of the effect of a given design parameter on the geoenvironmental performance of the liner. Secondly, they allow the designer to incorporate various uncertainties in the determination of these parameters. Such uncertainties can arise as a result of material heterogeneities, measurement imprecision or lack of site-specific data. Examples of such sources of uncertainty include spatial variability of the hydraulic conductivity of the attenuation layer, lack of data on the exact location of leakages and dependence of decay rates on variable physio-chemical conditions in the soil.

One of the advantages of characterising the performance of a landfill liner with leakage rates rather than chemical concentrations is that the former depends only on the hydraulic regime and not on the properties of specific contaminants. Hydraulic regimes in landfill liners can usually be determined and monitored with reasonable accuracy. However, it is obvious that a proper consideration of groundwater quality ought to be based on an assessment of chemical concentrations. This paper has shown that tools now exist to make the modelling exercise simpler and more accurate. However, the question of how the large number of possible contaminants can be incorporated in the design process remains open. A stochastic risk assessment philosophy, which takes into account the many uncertainties that are inherent to the modelling exercise and uses models such as SPAS or others, remains perhaps the best approach to the problem.

6 REFERENCES

Booker JR and Rowe RK. 1987. One dimensional advective-dispersive transport into a deep layer having a variable surface concentration. *International Journal of Numerical and Analytical Methods in Geomechanics* **11**(2): 131-142.

Canadian Council of Ministers of the Environment (CCME). 2007. Canadian Soil Quality Guidelines – Trichloroethylene – Environmental and Human Effects. CCME website: http://www.ccme.ca/assests/pdf/tce_ssd_1393.pdf (accessed 13 July 2009).

El-Zein A. 2003. Contaminant transport in fissured soils by three-dimensional boundary elements. *International Journal of Geomechanics ASCE,* **3**(1-2):75-83

El-Zein A. 2008. A generalized approach to the modelling of contaminant transport through intact and leaking geomembranes. *Intern. J Numer. and Analyti. Methods in Geomechanics,* **32**(3):265-287.

El-Zein A. and Rowe, R. K. 2008. Impact on groundwater of concurrent leakage and diffusion of dichloromethane through geomembranes in landfill liners. *Geosynthetics International*, **15** (1): 55-71.

Franca LP, Frey SL, Hughes TJR. 1992. Stabilized finite element methods: I. Application to the advective-diffusive model. *Computer Methods in Applied Mechanics and Engineering*, **95**:253-276.

Ogata A and Banks RB. 1961. A solution of the differential equation of longitudinal dispersion in porous media. *US Geological Survey*, Professions Paper 411-A.

Rowe RK, Quigley RM, Brachman RWI and Booker JR. 2004. *Barrier Systems for Waste Disposal Facilities*. 2nd Ed., Spon Press, London and New York.

Rowe RK and Booker JR. 1984. The analysis of pollutant migration in a non-homogeneous soil. *Geotechnique,* **34**(4):601-612.

Rowe RK. 2005. Long-term performance of contaminant barrier systems. *Geotechnique* **55(**9):631-678.

Rowe RK and Brachman RWI. 2004. Assessment of equivalency of composite liners, *Geosynthetics International,* **11**(4) 273-286.

Zienkiewicz OC, Taylor RL. 1991. *The Finite Element Method. Volume 2. Solid and Fluid Mechanics Dynamics and Non-Linearity.* McGraw-Hill Book Company: London, Fourth Edition, 1991; 461-484.